

A Jammed Parisi Ansatz

Michael Winer and Aidan Herderschee

Institute for Advanced Study, Princeton, NJ 08540, USA

Abstract

Constraint Satisfaction Problems are ubiquitous in fields ranging from the physics of solids to artificial intelligence. In many cases, such systems undergo a transition when the ratio of constraints to variables reaches some value α_{crit} . Above this critical value, it is exponentially unlikely that all constraints can be mutually satisfied. We calculate the probability that constraints can all be satisfied, $P(\text{SAT})$, for the spherical perceptron. Traditional replica methods, such as the Parisi ansatz, fall short. We find a new ansatz, the jammed Parisi ansatz, that correctly describes the behavior of the system in this regime. With the jammed Parisi ansatz, we calculate $P(\text{SAT})$ for the first time and match previous computations of thresholds. We anticipate that the techniques developed here will be applicable to general constraint satisfaction problems and the identification of hidden structures in data sets.

Contents

1	Introduction	2
2	The Parisi Ansatz in the Spherical Perceptron	4
2.1	Converting to the overlap matrix	4
2.2	Replica symmetric ansatz	6
2.3	Beyond replica symmetry	7
3	The Jammed Parisi Ansatz	8
3.1	The replica symmetric JPA	8
3.2	Replica symmetry breaking JPA	9
4	The Ground State Energy of the p-Spherical Model	11
5	Discussion	13
A	Details of Finding α_{crit}	17

1 Introduction

Constraint Satisfaction Problems (CSPs) are an important class of problems with applications ranging from physics to computer science to mathematics to artificial intelligence. The standard setup for such a problem is to have N primitive variables, which can be real numbers, binary variables, or something more exotic. One has some number of M of constraints on the N variables, each of which must be satisfied. One can ask questions such as whether there is an assignment of the variables which satisfies all of the constraints, and what such an assignment might be. More difficult questions include counting the full number of such satisfying assignments, and sampling the space of assignments efficiently.

The exponential size of the search space makes efficient general solutions to CSPs impossible. Boolean satisfiability, perhaps the single most famous CSP, is NP-complete. As are many other CSPs, including the ones studied in this paper. However, while solving an individual CSP is usually intractable, one valuable approach is the study of ensembles of CSPs. We can imagine drawing the constraints in our CSP from some specified distribution. Even if we cannot solve any individual instance, it is often feasible to prove statistical facts about the set of CSP with M constraints on N variables as $M, N \rightarrow \infty$.

A key quantity of interest is the probability, $P(\text{SAT})$, that a given CSP instance is satisfiable for a randomly chosen element of the distribution. Another fundamental concept is the *threshold*, often characterized by a critical value α_{crit} . Typically, $P(\text{SAT})$ is close to 1 when $\frac{M}{N} < \alpha_{\text{crit}}$ and close to 0 when $\frac{M}{N} > \alpha_{\text{crit}}$. Extensive research has been dedicated to determining α_{crit} for various CSPs, including Boolean satisfiability [1, 2, 3], the spherical perceptron [4, 5, 6, 7], and graph coloring [8]. In physics, these thresholds are conjectured to correspond to jamming transitions, where systems of hard grains reach a state beyond which further compression is impossible [6, 7]. Identifying the threshold is often a highly challenging problem. For instance, in the case of the spherical perceptron, it is believed that a full replica-symmetry-breaking calculation is required.

However, to our knowledge, very little has been done to calculate $P(\text{SAT})$ for almost any type of problem.¹ There are two motivations for such a calculation: threshold detection as above and

¹Ref. [9] is a notable exception.

structure detection in data sets. To study thresholds, one could calculate α_{crit} by seeing when instability develops in the $P(\text{SAT})$ computation. Regarding structure detection, Ref. [4] was the first to show how memorizing training data can be seen as a CSP. However, in real-life applications, the constraints are far from random, often leading to a vast increase in learnability [10, 11, 12, 13, 14, 15]. $P(\text{SAT})$ indicates the probability that an architecture could learn unstructured data. If $P(\text{SAT}) < 1$, we know that this data is unusually structured and that less than $P(\text{SAT})$ fraction of possible datasets is more learnable. One can then propose a structure for the data (say that the points all lie on a collection of low-dimensional manifolds) and calculate a new $P(\text{SAT})$ using these new constraints. If the new $P(\text{SAT})$ is still less than one, some additional structure is still to be understood.

To calculate $P(\text{SAT})$ for a system of constraints, we make use of the *Gardner volume* Z , the size of the solution space for a specific choice of the constraints. Since

$$\lim_{n \rightarrow 0} Z^n = \begin{cases} 0 & Z = 0 \\ 1 & Z > 0 \end{cases} \quad (1)$$

we have the identity

$$P(\text{SAT}) = \lim_{n \rightarrow 0} \overline{Z^n}. \quad (2)$$

Traditional replica calculations focus on systems like the p -spherical model or Sherrington-Kirkpatrick model where the limit $\lim_{n \rightarrow 0} \overline{Z^n}$ is identically 1, and the simplest interesting quantity is the free energy $\lim_{n \rightarrow 0} \partial_n \overline{Z^n}$. In this case, one can rely on calculations based on the Parisi Ansatz, described in [16, 17, 18, 19, 20, 21]. Unfortunately, the Parisi Ansatz will fail in cases where Z is often zero, because it cannot give a value of $\overline{Z^n}$ which is different from one. In cases like the overconstrained CSP, this manifests as an instability where $\partial_n \overline{Z^n}$ diverges. However, the jammed Parisi ansatz (JPA) is a generalized form of overlap matrix whose entries are allowed to depend on n . JPA overlap matrices are chosen so that $\lim_{n \rightarrow 0} \overline{Z^n}$ can be different from 1. For the replica symmetric JPA (RS JPA), this takes the form

$$Q_{ij} = \gamma n (\delta_{ij} - 1) + 1. \quad (3)$$

where Q_{ij} is the overlap matrix. Optimizing over JPA matrices, one can calculate $P(\text{SAT})$ for a wide variety of CSP. In fact, one can often get extremely precise values of $P(\text{SAT})$ with just the RS JPA.

Much of this note will focus on one of the simplest CSP: the *spherical perceptron*. Our constraints are a system of linear inequalities:

$$\begin{aligned} \vec{\xi}_\mu \cdot \vec{x} &> \sigma, \\ |\vec{x}| &= \sqrt{N} \end{aligned} \quad (4)$$

where \vec{x} is an N -dimensional vector to be determined and ξ_μ is a fixed N -dimensional vector for each $\mu = 1, \dots, M$. We will assume that each element of each ξ is drawn from Gaussian distributions with variance $\frac{1}{N}$, so that each ξ_μ is approximately a unit vector. The model has a long history, having been studied first in an artificial intelligence context, and also as a model of jamming transitions in physics [6, 22]. Ref. [4] showed that in the $\sigma = 0$ case, there is a phase transition when the ratio $\alpha = M/N$ reaches $\alpha_{\text{crit}} = 2$. For $\alpha > 2$, the system is over-constrained and $P(\text{SAT})$ is small. As M decreases below $2N$, the system becomes under-constrained, and $P(\text{UNSAT}) = 1 - P(\text{SAT})$ is small. We will compute the threshold of this transition, α_{crit} , as a function of σ along with $P(\text{SAT})$ using the JPA. For positive σ , the system is replica symmetric and our results do not differ from earlier work. For negative σ , where the system exhibits full replica symmetry breaking (RSB), the replica symmetric JPA still allows us to compute α_{crit} and $P(\text{SAT})$ to a high degree of precision.

One could calculate α_{crit} by computing $\lim_{n \rightarrow 0} \partial_n \overline{Z^n}$ using a Parisi ansatz, and seeing when the instability develops. We perform this calculation up to 2RSB, showing that it agrees exactly with the 1RBS Jammed Parisi Ansatz. However, the calculation using any level of the Parisi ansatz does not give $P(\text{SAT})$.

The plan for the paper is as follows. Section 2 is an overview of traditional replica methods as applied to the spherical perceptron. We derive the replicated action and get an expression for the satisfiability threshold in the replica symmetric cast.

Section 3 is the main technical meat of the paper: we derive the action for the spherical perceptron in the Jammed Parisi Ansatz, in both the replica symmetric and RSB cases. We calculate $P(\text{SAT})$, showing that even in the RS JPA it is a much lower threshold than the RS Parisi ansatz would predict, and examine the second-order nature of the transition.

Finally, in section 4 we consider another application of the JPA: the computation of ground-state energies. As a proof of concept, we compute the ground-state energy of the p -spherical model. To the authors' knowledge, the JPA ansatz is arguably the most efficient method for computing the ground state energies of disordered systems.²

2 The Parisi Ansatz in the Spherical Perceptron

The goal of this section is to review the standard approach to calculating α_{crit} for this system. This involves interpreting the size of solution space as a partition function, and then using the famous replica trick to calculate the free energy. In this section, we will review the setup of the calculation in terms of the replica trick. We will not perform a RSB analysis here; instead, we refer the reader to [7] for details.

2.1 Converting to the overlap matrix

The key quantity in our analysis of the linear system is

$$Z = \int_{S^N} d^N \vec{x} \prod_{\mu=1}^M \theta(\vec{\xi}_\mu \cdot \vec{x} - \sigma). \quad (5)$$

This quantity the volume of phase space that satisfies the M constraints, is often called the Gardner volume. Z is a random variable that depends on all $M \times N$ variables $\vec{\xi}_\mu$ which are drawn from a Gaussian ensemble

$$P(\vec{\xi}) = \frac{1}{\sqrt{2\pi\sigma^2}} e^{-\frac{\xi^2}{2\sigma^2}} \Big|_{\sigma=1/\sqrt{N}}. \quad (6)$$

If $Z = 0$, the system of inequalities is unsatisfiable. If Z is positive, the system of inequalities is satisfiable. The size of Z measures the size of the solution space for a given set of ξ s. \overline{Z} , the average value over the ξ s, gives the average size of solution space.

More important than \overline{Z} is $\overline{\log Z}$. When there is a large probability of Z being 0, this expectation becomes infinite. Thus, $\overline{\log Z}$ gives us a window into the transition to unsatisfiability. We use the replica trick to compute $\log \overline{Z}$.³ The philosophy behind this trick is explained extensively in the literature, see Refs. [24, 25, 26, 27]. We will attempt to give only a brief review. The fundamental idea is that the n th power of the partition function Z^n can be thought of as the partition function of a supersystem with n copies of the original system. One calculates the expected value of this

²Note that this computational strategy would not catch the failure of large- N perturbation theory described in Ref. [23].

³Note that $\overline{\log Z} \neq \log \overline{Z}$.

replicated partition function for general n , giving $\overline{Z^n}$. Then, if one is interested in $\overline{\log Z}$, one makes use of $\log Z = \partial_n Z^n|_{n=0}$, which we compute via saddle approximation in the large- N limit. To find the critical threshold, we find the critical ratio α_{crit} at which there is no valid saddle for $\overline{\log Z}$. Again, note that this method does not provide $P(\text{SAT})$ when $M/N > \alpha_{\text{crit}}$, but instead just computes the phase transition point α_{crit} .

To see this transition more explicitly, we compute $\overline{Z^n}$ as a function of the overlap matrix. We first note that the explicit ensemble averaged expression for $\overline{Z^n}$ is

$$\overline{Z^n} = \int \prod_i^n d^N \vec{x}_i \delta(\vec{x}_i^2 - N) \prod_\mu^M d^N \vec{\xi}_\mu P(\vec{\xi}_\mu) \theta(\vec{\xi}_\mu \cdot \vec{x}_i - \sigma) \quad (7)$$

where $P(\vec{\xi})$ is given in Eq. (6). For each $\vec{\xi}_\mu$ integral, we perform a change of variables.

$$\vec{\xi} = (h_1, \dots, h_n, \vec{\xi}_\perp), \quad \text{where } h_i = \vec{\xi} \cdot \vec{x}_i, \quad \vec{x}_i \cdot \vec{\xi}_\perp = 0 \quad (8)$$

and integrate over $\vec{\xi}_\perp$. Accounting for the Jacobian factor, the result is M products of

$$\begin{aligned} F(\vec{x}_i \cdot \vec{x}_j) &= \int d^N \vec{\xi}_\mu P(\vec{\xi}_\mu) \prod_i^n \theta(\vec{\xi}_\mu \cdot \vec{x}_i - \sigma) \\ &= \frac{1}{\sqrt{\det 2\pi(x_j \cdot x_i)}} \int d^n h_i e^{-\frac{1}{2} h_i (x_j \cdot x_i)^{-1} h_j} \prod_{i=1}^n \theta(h_i - \sigma). \end{aligned} \quad (9)$$

We then insert the overlap matrix $Q_{ij} = \vec{x}_i \cdot \vec{x}_j$ into the original integral

$$1 = \int d^{n \times n} Q_{ij} \delta(N Q_{ij} - \vec{x}_i \cdot \vec{x}_j) = \frac{1}{(4\pi)^{\frac{n(n+1)}{2}}} \int d^{n \times n} \Sigma_{ij} d^{n \times n} Q_{ij} e^{\frac{1}{2} \sum_{i \leq j} \Sigma_{ij} (N Q_{ij} - \vec{x}_i \cdot \vec{x}_j)} \quad (10)$$

exchange the delta function enforcing the spherical constraint with

$$\prod_i \delta(\vec{x}_i^2 - N) = \frac{1}{(2\pi)^n} \int d\lambda_i e^{\lambda_i (\vec{x}_i^2 - N)} \quad (11)$$

and finally integrate over \vec{x}_i . The end result is

$$\begin{aligned} \overline{Z^n} &= C \int d^{n \times n} Q d^{n \times n} \Sigma d^n \lambda \exp \left(M \log F(Q) - \frac{1}{2} N \log \Sigma + \frac{1}{2} N \sum_{i \leq j} \Sigma^{ij} Q_{ij} + N \sum_i \lambda_i (Q_{ii} - 1) \right) \\ \text{where } C &= \frac{(2\pi)^{-\frac{1}{2} n(n-N+3)}}{2^{\frac{n(n+1)}{2}}}. \end{aligned} \quad (12)$$

We are left with an integral in terms of Q , Σ , and λ . The contours for Σ and λ need to be the imaginary axis, perpendicular to the real line. Noticing that every term in the exponent is proportional to N , we can use the saddle-point method to solve Eq. (12). We will assume the saddle point formula is valid even in the $n \rightarrow 0$ limit. Importantly, one usually tries to find the Q which maximizes the log of the partition function, but the steepest descent contour actually minimizes the log for $n < 1$ [24, 25, 28]. Applying the saddle-point approximation at large- N , we solve the saddle point equations for Σ and λ , ultimately finding

$$\begin{aligned} \lim_{N \rightarrow \infty} \frac{\log(\overline{Z^n})}{N} &= \begin{cases} \max_Q \alpha \log F(Q) + \frac{1}{2} \text{tr} \log(Q) + \frac{n}{2} + \frac{n}{2} \log(2\pi) & \text{if } n \geq 1 \\ \min_Q \alpha \log F(Q) + \frac{1}{2} \text{tr} \log(Q) + \frac{n}{2} + \frac{n}{2} \log(2\pi) & \text{if } n < 1 \end{cases} \\ &\text{where } \forall_i : Q_{ii} = 1 \end{aligned} \quad (13)$$

We can now compute when there is a valid saddle approximation of \overline{Z}^n to study α_{crit} . For the remainder of the paper, we will assume we are working in the $N \rightarrow \infty$ limit and suppress the $\lim_{N \rightarrow \infty}$.

2.2 Replica symmetric ansatz

As an explanatory example, let us consider a replica symmetric ansatz compatible with the spherical constraint,

$$\forall 1 \leq i, j \leq n : \quad Q_{ij} = (1 - q)\delta_{ij} + q \quad (14)$$

which dominates for $\sigma > 0$. Every term in Eq. (13) is trivial to compute except $F(Q)$. To evaluate $F(Q)$, we add an auxiliary integration variable, h_0 and extend Q to

$$\forall i, j, \quad 0 \leq i, j \leq n : \quad Q'_{ij} = c\delta_{ij}(1 + \delta_{i0}q) + q \quad (15)$$

such that

$$\int \frac{d^n h_i}{\sqrt{\det 2\pi Q}} e^{-\frac{1}{2} \sum_{i,j} h_i (Q_{ij}^{-1}) h_j} \prod_{i=1}^n \theta(h_i - \sigma) = \int \frac{d^{n+1} h_i}{\sqrt{\det 2\pi Q'}} e^{-\frac{1}{2} \sum_{i,j} h_i (Q'_{ij}{}^{-1}) h_j} \prod_{i=1}^n \theta(h_i - \sigma) \quad (16)$$

and make the change of variables

$$\forall i, \quad 1 \leq i \leq n : \quad h_i = \delta h_i + h_0 . \quad (17)$$

The resulting integral drastically simplifies

$$F(Q) = \int \exp\left(-\frac{h_0^2}{2q}\right) \Theta\left(\frac{h_0 - \sigma}{\sqrt{1-q}}\right) \frac{dh_0}{\sqrt{2\pi q}} \quad (18)$$

where we define

$$\Theta(z) = \int_{-\infty}^z \exp\left(-\frac{h^2}{2}\right) \frac{dh}{\sqrt{2\pi}} \quad (19)$$

for convenience. In the limit $n \rightarrow 0$, we have

$$\lim_{n \rightarrow 0} \log F = n \int \exp\left(-\frac{h_0^2}{2q}\right) \log \Theta\left(\frac{h_0 - \sigma}{\sqrt{1-q}}\right) \frac{dh_0}{\sqrt{2\pi q}} \quad (20)$$

This is essentially a Gaussian integral of the log of the error function.

We do not care about computing $F(Q)$ for generic α , but instead near threshold. For $\alpha > \alpha_{\text{crit}}$ for some α_{crit} , Eq. (13) becomes arbitrarily negative as $q \rightarrow 1$ and has no saddle. This means that $\frac{1}{n} \log \overline{Z}^n$, the expected value of $\log Z$, now has an expectation value of negative infinity. This is precisely our phase transition, beyond which Z is zero with high probability. We wish to compute α_{crit} as an explicit function of σ . We make the approximation $q \sim 1$, which is valid for $\alpha \sim \alpha_{\text{crit}}$, and evaluate Eq. (20) analytically. We see that

$$\log \Theta\left(\frac{h_0 - \sigma}{\sqrt{1-q}}\right) \approx \begin{cases} -\frac{(h_0 - \sigma)^2}{2(1-q)}, & \text{if } h_0 - \sigma < 0 \\ 0, & \text{if } h_0 - \sigma > 0 \end{cases} \quad (21)$$

so

$$\log F \approx -\frac{1}{2(1-q)} \int_{-\infty}^{\sigma} \exp\left(-\frac{h_0^2}{2}\right) (\sigma - h_0)^2 \frac{dh_0}{\sqrt{2\pi}} = -\frac{K_1(\sigma)}{2(1-q)}, \quad (22)$$

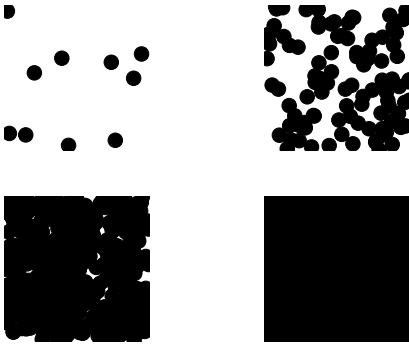


Figure 1: Each circle eliminates a small region of phase space, analogous to each constraint when σ is extremely negative. At low densities, the white region is connected. At higher densities, it shatters, until finally the black constraints cover every point.

where we define

$$K_1(\sigma) = \int_{-\infty}^{\sigma} \exp\left(-\frac{h_0^2}{2}\right) (\sigma - h_0)^2 \frac{dh_0}{\sqrt{2\pi}}. \quad (23)$$

Plugging this back into our action, we have

$$\frac{1}{N} \overline{\log Z} = \frac{1}{nN} \log \overline{Z^n} \approx \min_q \left(-\alpha \frac{K_1(\sigma)}{2(1-q)} + \frac{1}{2} \log(1-q) + \frac{1}{2} \left(\frac{q}{1-q} \right) - \frac{1}{2} \right). \quad (24)$$

We see that there is a phase transition at

$$\alpha_{\text{crit}} = \frac{1}{K_1(\sigma)}. \quad (25)$$

Whenever α is above this threshold, Eq. (24) has no local minimum, becoming arbitrarily negative as q approaches one.

2.3 Beyond replica symmetry

The RS Parisi ansatz in Eq. (25) is only valid for $\sigma > 0$. For $\sigma < 0$, one needs to use an ansatz that explicitly breaks replica symmetry. One important generalization is the k th-order RSB (k RSB) Parisi ansatz. In the k RSB ansatz, the $n \times n$ matrix is made out of blocks of size m_0 which is made out of blocks of size m_1 all the way down to blocks of size $m_k = 1$. Although we will not work through the details here, one can calculate both $\det Q$ and $F(Q)$ for this ansatz.

In order to build physical intuition, consider a 1RSB system whose saddle-point overlap matrix, Q , has some value of m between 0 and 1. The physical interpretation of this overlap matrix is that the allowed region of phase space has broken into disconnected blobs. Replicas in the same blob have overlap q_1 , replicas in different blobs have overlap $q_0 < q_1$.

For $\sigma > 0$, the region of the sphere satisfying all the constraints must always be simply connected and convex. This implies single region of phase space corresponds to a replica-symmetric saddle point for Q . By contrast, when $\sigma < 0$, each constraint cuts out just a small fraction of phase space (a share of about $e^{-\sigma^2/2}$). After enough small portions of phase space are removed, it becomes disconnected into multiple components. The components are blotted out one by one, and only then does the CSP become unsatisfiable. For negative σ , we expect the true saddles to display RSB.

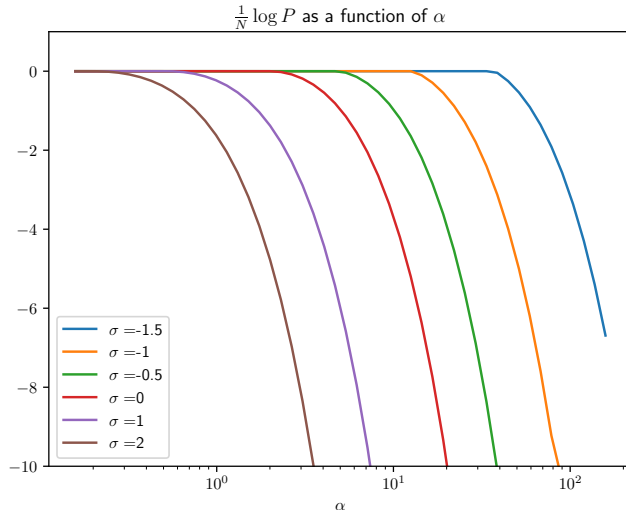


Figure 2: A graph of $\frac{1}{N} \log P(\text{SAT})$ as a function of α for various choices of σ . For larger values of σ , the transition appears to be second order. For the most negative values, one sees a discontinuity in the derivative at the transition point.

This explains why we expect the RS ansatz in Section 2.2 to fail. Since we are only analyzing a subset of Q s (the replica symmetric ones), we should expect the true value of \overline{Z}^n to be lower, and thus the Gardner volume should go to zero at an even lower value of α . This extremely complicated analysis was carried out in [29], and the authors got a value for α_{crit} identical to ours.

3 The Jammed Parisi Ansatz

The previous section focused on computing $\overline{\log Z}$. However, we want to compute $P(\text{SAT})$ directly, which is given by

$$P(\text{SAT}) = \lim_{n \rightarrow 0} \overline{Z}^n. \quad (26)$$

This probability might be close to 1 (if $\alpha < \alpha_{\text{crit}}$) or exponentially small (if $\alpha > \alpha_{\text{crit}}$). It is this phase transition, and what lies beyond it, that we will investigate in this section.

Interestingly, we find that the usual Parisi ansatz is insufficient. Instead, we must use a generalization of the Parisi ansatz, the JPA, where elements of Q_{ij} explicitly depend on n . We will give the RS JPA in Section 3.1. In Section 3.2, we give a k th-order replica symmetry breaking JPA (k RSB JPA) that is analogous to the k RSB Parisi ansatz. We believe the full JPA is necessary to reproduce the exact α_{crit} and $P(\text{SAT})$ for $\sigma < 0$, at least for the spherical perceptron. However, we find even the RS JPA is sufficient to get a very accurate result.

3.1 The replica symmetric JPA

We showed in section 2.2 that there is no fixed saddle point value of q in the $n \rightarrow 0$ limit for $\alpha > 1/K_1(\sigma)$. Instead, the action increases as q approaches one. This motivates us to introduce a new ansatz: $q = 1 - \gamma n$. More explicitly, the RS JPA is given by

$$\text{RS JPA : } Q_{ij} = \gamma n (\delta_{ij} - 1) + 1. \quad (27)$$

The calculation is formally the same as Section 2.2, except that there is additional n dependence. In particular,

$$\lim_{n \rightarrow 0} F(Q) = \log \int \frac{dh_0}{\sqrt{2\pi}} \exp\left(\frac{-h_0^2}{2}\right) \exp\left(-\frac{\min(h_0 - \sigma, 0)^2}{2\gamma}\right). \quad (28)$$

In the JPA, $\log \lim_{n \rightarrow 0} \overline{Z^n}$ has a fixed limit, not one proportional to n as with most thermodynamic systems. This limit is given by

$$\frac{1}{N} \log P(\text{SAT}) = \min_{\gamma} \left(\frac{1}{2} \log \left(\frac{\gamma + 1}{\gamma} \right) + \alpha \log \int \exp\left(-\frac{h_0^2}{2}\right) \exp\left(-\frac{\min(h_0 - \sigma, 0)^2}{2\gamma}\right) \frac{dh_0}{\sqrt{2\pi}} \right) \quad (29)$$

We can minimize Eq. (29) numerically. Results are plotted in Fig. 2. The first term in Eq. (29) is always positive and decreases towards 0 as γ increases. The integral term is always negative and increases towards 0. For small α , Eq. (29) is minimized by taking $\gamma \rightarrow \infty$ which sets Eq. (29) to zero, consistent with our finding in Section 2.2.

For larger α , the integral term will dominate, forcing a negative value of Eq. (29) at a finite value of γ . We can attempt a lower bound by noticing that $\log\left(\frac{\gamma+1}{\gamma}\right)$ is always positive and $\log \int \exp\left(-\frac{h_0^2}{2}\right) \exp\left(-\frac{\min(h_0 - \sigma, 0)^2}{2\gamma}\right) \frac{dh_0}{\sqrt{2\pi}}$ is always greater than $\log \int_{\sigma}^{\infty} \exp\left(-\frac{h_0^2}{2}\right) \frac{dh_0}{\sqrt{2\pi}}$, a negative number. Thus we have

$$\frac{1}{N} \log P(\text{SAT}) \geq \alpha \log \int_{\sigma}^{\infty} \exp\left(-\frac{h_0^2}{2}\right) \frac{dh_0}{\sqrt{2\pi}} \quad (30)$$

This lower bound corresponds exactly to the probability that any given point satisfies all the constraints. In other words, the probability that a CSP is satisfiable is lower-bounded by the probability that a given point satisfies all the constraints. This lower bound is a good approximation of $\log P(\text{SAT})$ at large α , as illustrated in Fig. 3. Even though this ansatz is replica symmetric, it gives different, seemingly more accurate answers than the vanilla RS calculation of the partition function we saw in Section 2.2.

One could wonder why we did not consider a q with more general n dependence. Let us assume a slightly more general ansatz

$$q = 1 - \gamma n^a \quad (31)$$

where $a > 0$. For $a < 1$, the $N \log(Q)$ in Eq. (13) vanishes in the limit that $n \rightarrow 0$ while $F(Q)$ is finite. Therefore, if there were a saddle, it would be independent of α , which is unphysical. In the case where $a > 1$, the $\log(Q)$ term diverges while the $F(Q)$ term is again finite, leading again to an unphysical result. Therefore, we are naturally led to $a = 1$.

Let us consider the physical interpretation of γ . For an allowed region of the \vec{x}_i phase space, the characteristic length scale is

$$i \neq j : \overline{(\vec{x}_i - \vec{x}_j)^2} = 2\gamma n. \quad (32)$$

Therefore, γ parametrizes how quickly the size of such regions goes to zero as n goes to zero.

3.2 Replica symmetry breaking JPA

The RS JPA has saddle points in the $n \rightarrow 0$ limit even in the unsatisfiable phase. Importantly, these saddle points have an action which remains constant as $n \rightarrow 0$. There are, however, more general ansatzes with this property. One, which inherits the structure of the k RSB Parisi ansatz described in Section 2.3, is the following.

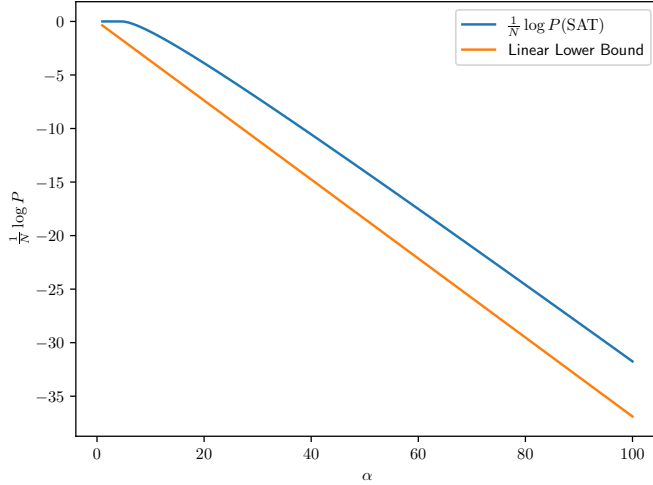


Figure 3: A plot with $\sigma = -0.5$ illustrating the true value of $\log P(\text{SAT})$ compared to the lower bound in equation 30. We see that it does indeed have the correct asymptotics for large α .

Eigenvalues	Degeneracy
γn	$n - \frac{1}{\tilde{m}_{k-1}}$
$(\gamma + (1 - q_{k-1})\tilde{m}_{k-1}) n$	$\frac{1}{\tilde{m}_{k-1}} - \frac{1}{\tilde{m}_{k-2}}$
\vdots	\vdots
$(\gamma + \sum_{i=0}^{k-1} (q_{i+1} - q_i)\tilde{m}_i) n$	1

Table 1: Eigenvalues of the RSB JPA.

The overlaps matrix consists of blocks of size $m_k = 1$ inside blocks of size $m_{k-1} < 1$ inside blocks of size $m_{k-2} < m_{k-1}$ all the way until a block of size $m_{-1} = n$. m_i is chosen to scale with n for $i < k$, going as $m_i = \tilde{m}_i n$. If a matrix element is inside a diagonal block of size m_i but not a diagonal block of size m_{i+1} , that element is q_{i+1} . We will choose all q_s to be fixed as $n \rightarrow 0$ except q_k , which goes as $1 - \gamma n$. The overlap distribution will be $1 - \gamma n$ with probability $\frac{1 - \tilde{m}_{k-1} n}{1 - n}$, which goes to 1 as n goes to 0. Thus, even though we have replica symmetry breaking, the chance that any two replicas are in the same minimum is 1, consistent with the idea that in the over constrained regime there is likely to be only one patch of phase space which satisfies all the constraints.

We can perform a calculation analogous to Section 3.1. The calculation of the log-determinant is fairly straightforward. The degeneracies of Q are given in Table 1. The calculation of the $\log(F(Q))$ is more cumbersome. However, we can repeat a similar trick as in Section 2.2 to find a recursive

expression for $F(Q)$

$$\begin{aligned}
g_k(h) &= \exp\left(-\frac{\min(h-\sigma, 0)^2}{2\gamma}\right) \\
g_i(h) &= \int_{-\infty}^{\infty} g_{i+1}(h')^{\frac{\tilde{m}_i}{\tilde{m}_{i+1}}} \exp\left(\frac{(h-h')^2}{2(q_{i+1}-q_i)}\right) \frac{dh'}{\sqrt{2\pi(q_{i+1}-q_i)}} \\
g_{-1}(h) &= \int_{-\infty}^{\infty} g_0(h')^{\frac{1}{\tilde{m}_0}} \exp\left(\frac{(h-h')^2}{2q_0}\right) \frac{dh'}{\sqrt{2\pi q_0}}.
\end{aligned} \tag{33}$$

where $F(Q) = g_{-1}(0)$, $\tilde{m}_k = 1$, and $q_k = 1$.

The full RSB JPA is cumbersome to work with, so instead we consider the $k = 1$ ansatz for simplicity. For $k = 1$, we can write everything in terms of three quantities: γ, q_0 and \tilde{m}_0 . The intensive action is

$$\begin{aligned}
S &= \frac{1}{2} \left(-\frac{1}{\tilde{m}_0} \log \gamma + \left(\frac{1}{\tilde{m}_0} - 1 \right) \log(\gamma + (1 - q_0)\tilde{m}_0) + \log(\gamma + (1 - q_0)\tilde{m}_0 + q_0) \right) \\
&+ \alpha \log \int_{-\infty}^{\infty} \exp\left(-\frac{h^2}{2q_0}\right) g(h)^{\frac{1}{\tilde{m}_0}} \frac{dh}{\sqrt{2\pi q_0}} \\
\text{where } g(h) &= \int_{-\infty}^{\infty} \exp\left(-\frac{\min(h'-\sigma, 0)^2 \tilde{m}_0}{2\gamma}\right) \exp\left(-\frac{(h-h')^2}{2(1-q_0)}\right) \frac{dh'}{\sqrt{2\pi(1-q_0)}}.
\end{aligned} \tag{34}$$

Now that we have Eq. (34) for the action, we need to minimize it with respect to γ, \tilde{m}_0 , and q_0 . For $\sigma > 0$, the action in Eq. (34) is minimized when $\tilde{m} = 1$ or $q_0 = 1$, corresponding to a replica symmetric matrix and giving us the same $P(\text{SAT})$ as in Section 3.1. However for any $\sigma < 0$, the minimum occurs at an RSB solution. We find the transition is always second-order in α . γ and \tilde{m} go as $(\alpha - \alpha_{\text{crit}})^{-1}$, meaning $\log P(\text{SAT})$ goes as $(\alpha - \alpha_{\text{crit}})^2$.

4 The Ground State Energy of the p -Spherical Model

The JPA isn't just useful for calculation capacities and thresholds. Since ground state energies can also be phrased as constraint satisfaction, the JPA can be used to calculate the location and large deviations of the ground state of a disordered system. The technique is to take $\lim_{n \rightarrow 0} \overline{Z_{\text{mic}}^n(E)}$, where $Z_{\text{mic}} = \int \delta(H(x) - E) d^N x$ is the microcanonical partition function, the total volume of configuration space at energy E . The limit $\lim_{n \rightarrow 0} Z_{\text{mic}}^n(E)$ is 0 if there are no configurations of energy E , and 1 if there are. Thus the disorder average is precisely the probability that there are configurations at energy E . When it first dips below 1, we are below the quenched ground state energy.

This technique appears to work for a wide variety of disordered systems, but we will demonstrate it here for the p -spherical model [30, 31, 32, 33, 34, 35, 36]. This is a simple statistical mechanical model with

$$H(x) = \sum_{1 \leq i_1 \leq i_2 \dots \leq i_p \leq N} J_{i_1 i_2 \dots i_p} x_{i_1} x_{i_2} \dots x_{i_p}, \tag{35}$$

that is a random p th order potential with coefficients chosen from an iid normal distribution with variance $\frac{p!}{N^{p-1}}$. The word ‘‘spherical’’ in the model’s name refers to the spherical condition

$$\sum_{i=1}^n x_i^2 = N. \tag{36}$$

σ	RS PA	RS JPA	1RSB JPA
-3.0	4915.573	2526.293	2526.143
-2.9	3390.300	1803.603	1803.416
-2.8	2358.003	1298.765	1298.540
-2.7	1653.743	943.216	942.944
-2.6	1169.455	690.775	690.447
-2.5	833.804	510.098	509.707
-2.4	599.351	379.757	379.295
-2.3	434.317	284.989	284.453
-2.2	317.256	215.553	214.940
-2.1	233.592	164.287	163.601
-2.0	173.348	126.152	125.402
-1.9	129.646	97.573	96.775
-1.8	97.711	76.001	75.173
-1.7	74.205	59.599	58.763
-1.6	56.779	47.041	46.218
-1.5	43.769	37.360	36.567
-1.4	33.989	29.845	29.098
-1.3	26.586	23.973	23.285
-1.2	20.944	19.354	18.735
-1.1	16.616	15.698	15.153
-1.0	13.273	12.784	12.320
-0.9	10.676	10.448	10.066
-0.8	8.644	8.563	8.264
-0.7	7.045	7.031	6.816
-0.6	5.779	5.779	5.648
-0.5	4.770	4.770	4.700
-0.4	3.962	3.962	3.928
-0.3	3.311	3.311	3.297
-0.2	2.783	2.783	2.779
-0.1	2.353	2.353	2.352
0.0	2.000	2.000	2.000

Table 2: Critical values of α for different σ values. The first column is the replica symmetric Parisi answer from equation 25. Column 2 a the replica-symmetric JPA, which we find gives precisely the same answer as the 1RSB Parisi ansatz. This answer differs significantly from the simple RS Parisi Ansatz. Column 3 is the 1RSB JPA value for α_{crit} , nearly the same as RS JPA.

Because the J s are all Gaussian random variables, the joint distribution of any collection of points will be jointly Gaussian with covariance

$$\overline{H(x_\alpha)H(x_\beta)} = Nq_{\alpha\beta}^p. \quad (37)$$

The replicated microcanonical partition function is

$$\overline{Z_{\text{mic}}^n(E)} = \overline{\int d^n x \int d^n \lambda \exp\left(\sum_{\alpha=1}^n \Lambda_\alpha(H(x_\alpha) - E)\right)}. \quad (38)$$

We can perform the Gaussian integral to get

$$\overline{Z_{\text{mic}}^n(E)} = \int d^n x \int d^n \lambda \exp\left(\frac{N}{2} \sum_{\alpha,\beta=1}^n \lambda^2 q_{\alpha\beta}^p - n \sum_{\alpha=1}^n \Lambda_\alpha E\right). \quad (39)$$

Integrating out the x s, we are left with

$$\log \overline{Z_{\text{mic}}^n(E)} = \frac{N}{2} \log \det q + \frac{N}{2} \sum_{\alpha=1}^n \lambda^2 q_{\alpha\beta}^p - n \Lambda E. \quad (40)$$

We will assume a replica-symmetric JPA for the matrix q , and let Λ scale as L/n . Under this ansatz

$$\begin{aligned} \log \det q &= \log \frac{1+\gamma}{\gamma} \\ \sum_{\alpha\beta} \lambda_\alpha \lambda_\beta q_{\alpha\beta}^p &= pL^2\gamma \end{aligned} \quad (41)$$

This gives us the action

$$\frac{1}{N} \log \overline{Z_{\text{mic}}^n(E)} = \frac{1}{2} \log \frac{1+\gamma}{\gamma} + \frac{1}{2}(1+p\gamma)L^2 - LE. \quad (42)$$

We can solve for L and get $L = \frac{E}{p\gamma}$, giving us

$$\frac{1}{N} \log \overline{Z_{\text{mic}}^n(E)} = \min_{\gamma} \left(\frac{1}{2} \log \frac{1+\gamma}{\gamma} - \frac{E^2}{2(1+p\gamma)} \right). \quad (43)$$

For, say $p = 3$, this becomes negative at $E = -1.6569983$, precisely the point that replica thermodynamics predicts. Since the p -spherical model is a 1RSB-exact system, the fact that the RS JPA gets precisely the correct answer might lead to a conjecture that the k -level JPA somehow contains the same information as the $k+1$ -level Parisi Ansatz. Unfortunately this doesn't seem to be borne out: for mixed p -spin models such as the ones in [37], this conjecture appears to be false and the k th order JPA seems to contain the same information as k RSB Parisi. Working out a general principle behind these correspondences would be an interesting direction for future work.

5 Discussion

In this letter, we computed $P(\text{SAT})$ and α_{crit} for the spherical perceptron using a novel generalization of the Parisi ansatz. For $\sigma > 0$, we found that the RS JPA accurately predicted $P(\text{SAT})$ and α_{crit} in the large- N limit. For $\sigma < 0$, we conjectured that a RSB JPA would yield the exact values

of $P(\text{SAT})$ and α_{crit} , though we only explicitly evaluated the 1RSB JPA. While the 1RSP JPA produced results differing from the RS JPA, the discrepancy in α_{crit} was less than 0.01%, indicating that the RS JPA is a good approximation for $P(\text{SAT})$ and α_{crit} .

One important collection of results has to do with the order of the transition in $P(\text{SAT})$. Once we introduce replica symmetry breaking in the JPA, we find that the transition is second order for all values of σ , meaning that $\log P(\text{SAT}) \sim (\alpha - \alpha_{\text{crit}})^2$. This suggests that for respectably large values of N , one can add $O(\sqrt{N})$ more constraints above the threshold before the satisfaction probability is significantly diminished.

By comparison, the transition appears to be first order in the context of the p -spherical model. Furthermore, since the RS JPA gets the location of the transition exactly right, and if the RS solution gives $\log P(E) \sim (E - E_{\text{crit}})^1$, then no higher-order ansatz can give a less negative value of P such as $(E - E_{\text{crit}})^2$. Explaining why the p -spherical model has qualitatively different behavior than the spherical perceptron for both positive and negative σ is an open question.

Interestingly, in certain circumstances, the JPA can be used to investigate $P(\text{UNSAT}) = 1 - P(\text{SAT})$ deep in the satisfiable phase. When the CSP corresponds to a convex optimization problem (as occurs in the spherical perceptron when $\sigma \geq 0$), the unsatisfiability of the CSP is dual to the satisfiability of some other CSP. By applying the JPA to this dual problem, we can calculate the exponentially small difference between $P(\text{SAT})$ and 1 for certain CSPs in the satisfiable regime.

Another promising avenue for investigation is the distribution of gaps, whose significance has been emphasized in Refs. [38, 7]. These works primarily focused on the gap distribution of random CSPs in the UNSAT phase, providing insight into how close such elements were to satisfiability. In contrast, an analysis of $\lim_{n \rightarrow 0} \overline{Z}^n$ using the JPA conditions to the satisfiable instances of the CSP. This suggests that applying the methods of Refs. [38, 7] in this context could yield the gap distribution for satisfiable elements, possibly giving some insight as to what happens when jammed systems are given time to anneal.

Finally, the tools of the JPA in hand, a natural next target is more structured satisfiability problems, such as classifying neural manifolds [13, 15], or even data with covariances given by a colored Gaussian rather than the identity.

Acknowledgments

We thank Jaron Kent-Dobias, Jonah Kudler-Flam and Vladimir Narovlansky for useful discussions. MW acknowledges DOE grant DE-SC0009988. AH is grateful to the Simons Foundation as well as the Edward and Kiyomi Baird Founders' Circle Member Recognition for their support.

References

- [1] Marc Mézard, Giorgio Parisi, and Riccardo Zecchina, “Analytic and algorithmic solution of random satisfiability problems,” *Science* **297**, 812–815 (2002)
- [2] Marc Mézard and Riccardo Zecchina, “Random k-satisfiability problem: From an analytic solution to an efficient algorithm,” *Physical Review E* **66** (Nov. 2002), ISSN 1095-3787, doi:\bibinfo{doi}{10.1103/physreve.66.056126}, <http://dx.doi.org/10.1103/PhysRevE.66.056126>
- [3] Dimitris Achlioptas, Assaf Naor, and Yuval Peres, “On the maximum satisfiability of random formulas,” (2003), [arXiv:math/0305151 \[math.PR\]](https://arxiv.org/abs/math/0305151), <https://arxiv.org/abs/math/0305151>

- [4] E. Gardner and B. Derrida, “OPTIMAL STORAGE PROPERTIES OF NEURAL NETWORK MODELS,” *J. Phys. A* **21**, 271 (1988)
- [5] E. Gardner, “The space of interactions in neural network models,” *Journal of Physics A* **21**, 257–270 (1988), <https://api.semanticscholar.org/CorpusID:15378089>
- [6] Silvio Franz and Giorgio Parisi, “The simplest model of jamming,” *Journal of Physics A: Mathematical and Theoretical* **49**, 145001 (Feb. 2016), ISSN 1751-8121, <http://dx.doi.org/10.1088/1751-8113/49/14/145001>
- [7] Silvio Franz, Giorgio Parisi, Maxime Sevelev, Pierfrancesco Urbani, and Francesco Zamponi, “Universality of the sat-unsat (jamming) threshold in non-convex continuous constraint satisfaction problems,” *SciPost Physics* **2** (Jun. 2017), ISSN 2542-4653, doi:\bibinfo{doi}{10.21468/scipostphys.2.3.019}, <http://dx.doi.org/10.21468/SciPostPhys.2.3.019>
- [8] A. Frieze and M. Molloy, “The satisfiability threshold for randomly generated binary constraint satisfaction problems,” in *Approximation, Randomization, and Combinatorial Optimization: Algorithms and Techniques. RANDOM APPROX 2003*, Lecture Notes in Computer Science, Vol. 2764, edited by S. Arora, K. Jansen, J.D.P. Rolim, and A. Sahai (Springer, Berlin, Heidelberg, 2003)
- [9] Leonardo Cruciani, “On the capacity of neural networks,” (2022), [arXiv:2211.07531 \[cond-mat.dis-nn\]](https://arxiv.org/abs/2211.07531), <https://arxiv.org/abs/2211.07531>
- [10] Francesca Mignacco, Chi-Ning Chou, and SueYeon Chung, “Nonlinear classification of neural manifolds with contextual information,” (2024), [arXiv:2405.06851 \[q-bio.NC\]](https://arxiv.org/abs/2405.06851), <https://arxiv.org/abs/2405.06851>
- [11] Chi-Ning Chou, Luke Arend, Albert J. Wakhloo, Royoung Kim, Will Slatton, and SueYeon Chung, “Neural manifold capacity captures representation geometry, correlations, and task-efficiency across species and behaviors,” *bioRxiv*(2024), doi:\bibinfo{doi}{10.1101/2024.02.26.582157}, <https://www.biorxiv.org/content/early/2024/02/28/2024.02.26.582157.full.pdf>, <https://www.biorxiv.org/content/early/2024/02/28/2024.02.26.582157>
- [12] Albert J. Wakhloo, Tamara J. Sussman, and SueYeon Chung, “Linear classification of neural manifolds with correlated variability,” *Phys. Rev. Lett.* **131**, 027301 (Jul 2023), <https://link.aps.org/doi/10.1103/PhysRevLett.131.027301>
- [13] S. Chung, D. D. Lee, and H. Sompolinsky, “Linear readout of object manifolds,” *Physical Review E* **93**, 060301 (2016)
- [14] U. Cohen, S. Chung, D. D. Lee, and H. Sompolinsky, “Separability and geometry of object manifolds in deep neural networks,” *Nature Communications* **11**, 746 (2020)
- [15] S. Chung, D. D. Lee, and H. Sompolinsky, “Classification and geometry of general perceptual manifolds,” *Physical Review X* **8**, 031003 (2018)
- [16] G. Parisi, “Infinite number of order parameters for spin-glasses,” *Phys. Rev. Lett.* **43**, 1754–1756 (Dec 1979), <https://link.aps.org/doi/10.1103/PhysRevLett.43.1754>
- [17] Giorgio Parisi, “A sequence of approximated solutions to the s-k model for spin glasses,” *Journal of Physics A: Mathematical and General* **13**, L115–L121 (1980)

- [18] Giorgio Parisi, “Order parameter for spin-glasses,” *Physical Review Letters* **50**, 1946–1948 (1983)
- [19] Marc Mézard, Giorgio Parisi, and Miguel Angel Virasoro, *Spin glass theory and beyond* (World Scientific Publishing, 1987) ISBN 978-9971501150
- [20] Michel Talagrand, “The parisi formula,” *Annals of Mathematics* **163**, 221–263 (2006)
- [21] Dmitry Panchenko, *The Sherrington-Kirkpatrick model*, Springer Monographs in Mathematics (Springer, 2013) ISBN 978-1461470906
- [22] Claudia Artiago, Federico Balducci, Giorgio Parisi, and Antonello Scardicchio, “Quantum jamming: Critical properties of a quantum mechanical perceptron,” *Physical Review A* **103** (Apr. 2021), ISSN 2469-9934, doi:\bibinfo{doi}{10.1103/physreva.103.l040203}, <http://dx.doi.org/10.1103/PhysRevA.103.L040203>
- [23] Aidan Herderschee and Michael Winer, “Failure of the large-N expansion in a Bosonic Tensor Model,” (10 2024), [arXiv:2410.06896 \[hep-th\]](https://arxiv.org/abs/2410.06896)
- [24] Tommaso Castellani and Andrea Cavagna, “Spin-glass theory for pedestrians,” *Journal of Statistical Mechanics: Theory and Experiment* **2005**, P05012 (May 2005), ISSN 1742-5468, <http://dx.doi.org/10.1088/1742-5468/2005/05/P05012>
- [25] Marc Mézard, Giorgio Parisi, M. A. Virasoro, and David J. Thouless, “Spin glass theory and beyond,” (1987) <https://api.semanticscholar.org/CorpusID:120860082>
- [26] K. H. Fischer and J. A. Hertz, *Spin Glasses*, Cambridge Studies in Magnetism (Cambridge University Press, 1991)
- [27] Cirano De Dominicis and Irene Giardina, *Random Fields and Spin Glasses: A Field Theory Approach* (Cambridge University Press, 2006)
- [28] Bernard Derrida and Peter Mottishaw, “Finite size corrections in the random energy model and the replica approach,” *Journal of Statistical Mechanics: Theory and Experiment* **2015**, P01021 (Jan. 2015), ISSN 1742-5468, <http://dx.doi.org/10.1088/1742-5468/2015/01/P01021>
- [29] Brandon L. Annesi, Enrico M. Malatesta, and Francesco Zamponi, “Exact full-rsb sat/unsat transition in infinitely wide two-layer neural networks,” (2025), [arXiv:2410.06717 \[cond-mat.dis-nn\]](https://arxiv.org/abs/2410.06717), <https://arxiv.org/abs/2410.06717>
- [30] Andrea Cavagna, Irene Giardina, and Giorgio Parisi, “Stationary points of the Thouless-Anderson-Palmer free energy,” *Phys. Rev. B* **57**, 1123612–11257 (04 1998)
- [31] A. Crisanti, H. Horner, and H. J. Sommers, “The spherical p-spin interaction spin-glass model,” *Z. Phys. B* **92**, 257–271 (Jun 1993)
- [32] A. Crisanti and H. Sommers, “Thouless-Anderson-Palmer approach to the spherical p-spin spin glass model,” *J. Phys., I* **5**, 805–813 (Jul 1995)
- [33] Leticia F. Cugliandolo and Gustavo Lozano, “Real-time nonequilibrium dynamics of quantum glassy systems,” *Phys. Rev. B* **59**, 915–942 (Jan 1999)
- [34] L. F. Cugliandolo and J. Kurchan, “Analytical solution of the off-equilibrium dynamics of a long-range spin-glass model,” *Phys. Rev. Lett.* **71**, 173–176 (Jul 1993)

- [35] Luca D’Alessio, Yariv Kafri, Anatoli Polkovnikov, and Marcos Rigol, “From quantum chaos and eigenstate thermalization to statistical mechanics and thermodynamics,” *Adv. Phys.* **65**, 239–362 (2016)
- [36] Prabodh Shukla and Surjit Singh, “Classical and quantum spherical models of spin-glasses: A complete treatment of statistics and dynamics,” *Phys. Rev. B* **23**, 4661–4666 (May 1981), <https://link.aps.org/doi/10.1103/PhysRevB.23.4661>
- [37] Antonio Auffinger and Qiang Zeng, “Existence of two-step replica symmetry breaking for the spherical mixed p-spin glass at zero temperature,” *Communications in Mathematical Physics* **370**, 377–402 (Sep. 2018), ISSN 1432-0916, <http://dx.doi.org/10.1007/s00220-018-3252-3>
- [38] Matthieu Wyart, “Marginal stability constrains force and pair distributions at random close packing,” *Phys. Rev. Lett.* **109**, 125502 (Sep 2012), <https://link.aps.org/doi/10.1103/PhysRevLett.109.125502>

A Details of Finding α_{crit}

The jammed phase corresponds precisely to cases where $\log P(\text{SAT})$ is negative. That is, for any value of α and σ where the minimum of action 12 over JPA matrices is negative, the spherical perceptron is jammed. Since the action is of the form

$$S = \text{determinant term} + \alpha * \text{integral term}, \quad (44)$$

the phase transition happens at

$$\alpha_{\text{crit}} = \min_Q \frac{-\text{determinant term}}{\text{integral term}} \quad (45)$$

The special Q where this minimum ratio happens is also the saddle-point matrix for α just above α_{crit} . As α increases further, the saddle-point can move.

For the replica symmetric JPA, the minimization process just boils down to minimizing over one number, γ . There is a small subtlety for $\sigma > \sigma^* \approx -0.6129\dots$. This minimum occurs at $\gamma = \infty$, but the minimum occurs at finite γ for $\sigma < \sigma^*$. This means that the transition occurs in a region where both terms themselves (which scale as γ^{-1}) are zero for $\sigma > \sigma^*$, so $\frac{dS}{d\alpha}|_{\alpha_{\text{crit}}} = 0$. In contrast, $\frac{dS}{d\alpha}|_{\alpha_{\text{crit}}} = 0$ is negative and the transition appears first-order within the replica symmetric ansatz for $\sigma < \sigma^*$.

For the RSB JPA, the situation is more complex. Theoretically, we still only need to minimize the ratio of terms over all sets of γ , q_0 and \tilde{m} . The minimum now occurs when γ, \tilde{m} go to infinity with their ratios fixed. This brings us to a similar situation to the case of the RS JPA with $\sigma > \sigma^*$, where both the determinant and integral terms of the action are zero at α_{crit} , so the transition is second-order.